

DEL-SG-30-89

**An Approximation Scheme For The
Three-dimensional Scattered Wave And Its
Propagating Far-field Pattern In A Finite
Depth Ocean**

\$2.00

by

Robert P. Gilbert
Dept. of Math. Sciences
University of Delaware
Newark, DE 19716, USA

Yongzhi Xu
Dept. of Math. Sciences
University of Delaware
Newark, DE 19716, USA

Peter Thejll
Dept. of Physics & Astronomy
University of Delaware
Newark, DE 19716, USA

October 1989

University of Delaware Sea Grant College Program
Newark, DE 19716

This publication is the result of research sponsored by NOAA Office of Sea Grant, Department of Commerce, under Grant No. NA86AA-D-SG040 (Project No. R/OE-2). The U.S. Government is authorized to produce and distribute reprints for governmental purposes, notwithstanding any copyright notation that may appear hereon.

The University of Delaware Sea Grant College Program is supported cooperatively by the National Oceanic and Atmospheric Administration, U.S. Department of Commerce, and by the State of Delaware.

An Approximation Scheme For The Three-dimensional Scattered Wave And Its Propagating Far-field Pattern In A Finite Depth Ocean

R. P. Gilbert and Yongzhi Xu
Dept. of Math. Sciences ,
Peter Thejll
Dept. of Physics and Astronomy,
University of Delaware ,
Newark , DE 19716 . ¹

1. Introduction

This paper may be considered STEP ONE in a sequence dedicated to solving the *submersible identification problem*. Our method is based on an approach used by Colton and Monk[6][7] for similar problems using radar in space(R^2 , or R^3). Our problem is much more difficult. First we have an index of refraction which depends, at least, on depth, and perhaps also on range. Second our domain is not all of space but an “irregular slab”. In the first approach we shall concentrate on an ocean which is a slab of thickness h , R_h^3 , and has a constant index of refraction, as the most disturbing aspect of our problem appears to be the way the ocean surface interfere with the propagation of sound.

In STEP ONE we shall concentrate on an efficient numerical scheme to compute the far field generated by scattering a generalized plane wave off

¹This work is supported in part by Sea Grant NA86AA-D-SG040.

an arbitrary submersible. Subsequent papers will deal with reconstruction of the object from the far field , and how to introduce the effect of a variable index of refraction using transmutation theory. We shall outline our approach to the entire problem in this introduction. The remainder of the paper, however, shall deal only with the computational aspects of STEP ONE.

Because of the interference of the ocean surface analytical computation of the far field must take into account some sort of approximation scheme, such as using parabolic approximation, which tends to destroy vertical resolution or using a truncated form of the modal expansion for the Green's function (propagator):

$$G(r, z; \rho, \zeta) = \sum_{n=0}^{\infty} \frac{\phi_n(z)\phi_n(\zeta)}{\|\phi_n\|^2} H_0(ka_n | re^{i\theta} - \rho e^{i\phi} |). \quad (1.1)$$

Here the $a_n = [1 - (n + 1/2)^2(\pi/kh)^2]^{-1/2}$ are the modal eigenvalues [1]. For the case of a variable index ocean a similar expansion is available where the modal functions $\phi_n(z)$ and their corresponding eigenvalues may be obtained through transmutation as been done by Dustin, Gilbert, Wood, and Verma[8]. By using the propagator $G(r, z; \rho, \zeta)$ (1.1), the Green's integral representation, and the asymptotic behavior of the Hankel functions, Gilbert and Xu[2] have shown that the acoustic pressure to have the asymptotic expansion

$$\begin{aligned} p(r, z, \theta) &= \frac{1}{r^{1/2}} \sum_{n=0}^{\infty} e^{ika_n r} \sum_{m=0}^{\infty} \frac{f_{nm}(z, \theta)}{r^m} \\ &\simeq \frac{1}{r^{1/2}} \sum_{m=0}^{\infty} \frac{F_m(r, z, \theta)}{r^m}, \end{aligned} \quad (1.2)$$

where

$$F_m(r, z, \theta) := \sum_{n=0}^N e^{ika_n r} F_{nm}(z, \theta). \quad (1.3)$$

The modes $\phi_n(z)$ for $n > N$ do not propagate, but rather decay exponentially and hence do not appear in the sum (1.3). We refer to the term

$$F_0(r, z, \theta) := \sum_{n=0}^N e^{ika_n r} F_{n0}(z, \theta). \quad (1.4)$$

as the finite-ocean far field pattern, which we also write in an array form as

$$F(z, \theta) := [f_{00}(z, \theta), f_{10}(z, \theta), \dots, f_{N0}(z, \theta)].$$

By the use of Green's formula it is possible to establish the identity [8]

$$A_N D_N(r) F(z, \theta) = \sqrt{\frac{2}{i\pi k}} V_N D_N(r) \int_{\partial D} \frac{\partial u(\xi, \zeta)}{\partial \nu_\xi} G(\mathbf{x}, z, \xi, \zeta) d\sigma_\xi,$$

where \mathbf{x} and ξ are two-dimensional vectors in the range plane, and A_N is the $(N+1) \times (N+1)$ Vandermonde matrix of constant coefficients

$$A_N := \begin{bmatrix} 1 & 1 & \dots & 1 \\ ika_0 & ika_1 & \dots & ika_N \\ \vdots & \vdots & \ddots & \vdots \\ (ika_0)^N & (ika_1)^N & \dots & (ika_N)^N \end{bmatrix},$$

and $D_N(r)$ is the $(N+1) \times (N+1)$ diagonal matrix

$$D_N(r) := \text{diag} [e^{ika_0 r}, e^{ika_1 r}, \dots, e^{ika_N r}] \quad (1.5)$$

The array $\Psi(\mathbf{x}, z, \xi, \zeta)$ is given by

$$\Psi := \left[\frac{e^{ika_0 \langle \mathbf{x}, \xi \rangle}}{\|\phi_0\|^2 \sqrt{a_0}} \phi_0(z) \phi_0(\zeta), \dots, \frac{e^{ika_N \langle \mathbf{x}, \xi \rangle}}{\|\phi_N\|^2 \sqrt{a_N}} \phi_N(z) \phi_N(\zeta) \right] \quad (1.6)$$

This leads to the following integral representation for the far field pattern generated by reflection off a submersible with boundary ∂D

$$F(z, \theta) = \sqrt{\frac{2}{i\pi k}} \int_{\partial D} \frac{\partial u(\xi, \zeta)}{\partial \nu_\xi} \Psi(\mathbf{x}, z, \xi, \zeta) d\sigma_\xi, \quad (1.7)$$

Gilbert and Xu [2] show that the propagating solutions therefore have a modal representation of form

$$\nu(\mathbf{x}, z) := \sum_{n=0}^N \frac{\phi_n(\zeta)}{\|\phi_n\|^2 \sqrt{a_n}} \int_{\partial Z_1} g(z, \phi) \phi_n(z) e^{ik a_n \langle \mathbf{x}, \xi \rangle} d\sigma_\xi. \quad (1.8)$$

Equation (1.8) indicates that the information received from the far-field must be incomplete; consequently, the problem of trying to determine the shape of the submersible from far field data is really an *ill-posed problem*. In order to extract some information it is necessary to restrict the space of solutions somehow in order to make the problem *well-posed*. There are several possibilities which seem quite promising. One possibility is to seek the solution among all objects of a general size and shape, for example an ellipsoid. Since the number of modes which propagate depends on the wave number it is import to keep the wave number sufficiently high, i.e. so that 10 to 20 modes actually propagate.

One way to generate the starting field is to essentially ignore the interference from the ocean surface. This is a reasonable assumption providing the ocean is deep enough and the source not close to either surface. In this instance, we may assume, in the case of a constant index ocean, that the local situation is governed by a spherical geometry, and that a complete family of solutions is given by

$$\left\{ \Phi_n(\rho, \theta, \phi) := H_{n+1/2}^{(1)}(k\rho) P_n^m(\cos\theta) e^{im\phi} \right\}, \quad n = 0, 1, 2, \dots, \quad (1.9)$$

$m = 0, \pm 1, \pm 2, \dots, \pm n$, where $\rho^2 = (z - z_0)^2 + r^2$, and $\theta = \cos^{-1}(z/\rho)$. $H_{n+1/2}^{(1)}(\zeta)$ is a spherical Hankel function and is usually denoted by $h_n^{(1)}(\zeta)$. The starting field is then written as a finite sum of functions from the class (1.9) such

that on the surface of the object the soft sound boundary condition is approximated. This condition may be formulated as a minimization problem.

The approximate starting field is given in the form

$$u(\rho, \theta, \phi) := \sum_{n=0}^N \sum_{m=-n}^n \tau_n h_n^{(1)}(k\rho) P_n^m(\cos\phi) e^{im\theta} \quad (1.10)$$

In order to obtain the propagating field we must match the starting field with a sum of the propagating modes in a region where both approximations are valid, i.e. we attempt to seek the coefficients β_{nm} in the series

$$\sum_{n=0}^{N_2} \sum_{m=-M}^M \beta_{mn} \cos[k(1-a_n^2)^{1/2}(h-z)] H_m^1(ka_n r) e^{im\theta} \quad (1.11)$$

The computation of the coefficients β_{nm} and the display of the far-field, using the asymptotic expansions for the Hankel functions, as a series

$$u(\rho, \theta, \phi) \simeq \sqrt{\frac{2}{ik\pi}} \sum_{n=0}^{N_2} \sum_{m=-M}^M \beta_{mn} r^{-1/2} e^{i(ka_n r - m\pi/2)} \cos[k(1-a_n^2)^{1/2}(h-z)] H_m^1(ka_n r) e^{im\theta}, \quad (1.12)$$

concludes STEP ONE in our procedure.

STEP TWO

Having obtained an approximate far field pattern, for various wave numbers k and various z dependencies in the incident “plane waves”, we may now try to solve the inverse problem. Recall that the “plane waves” have modal components in the z direction. If we are not considering an axially symmetric solutions then for each modal component and for each k we use $2n+1$ incoming waves with directions in the range coordinates

$$\mathbf{a}_2^j = [\cos(2\pi j/(2n+1)), \sin(2\pi j/(2n+1))], \quad j = 0, 1, 2, \dots, 2n \quad (1.13)$$

Now let F_{nm}^j $0 \leq n \leq N$, $-n \leq m \leq n$ be the coefficients of the spherical harmonic approximation of far field pattern F^j generated by the plane wave

with the direction $\alpha_2^{(j)}$. By expanding the propagating Herglotz kernels, and the parametric representation of the submersible's surface $\rho = f(\theta, \phi)$ in terms of the surface harmonics we are led, for example, to consider a minimization problem of the form

$$\begin{aligned} \mu(F) = \min_{(k^2, g, \rho)} & \left\{ \sum_{j=1}^{2n} \left| \int_{\partial Z_1} F(z, \phi; k, \alpha_2^{(j)}) g(z, \phi) dz d\phi \right|^2 \right. \\ & \left. + \int_0^{2\pi} \int_0^\pi |T^{-1}V(f(\phi, \theta), \phi, \theta)|^2 \sin^2 \theta d\theta d\phi \right\}, \end{aligned} \quad (1.14)$$

where

$$V(y) := \sqrt{\frac{2}{ik\pi}} \int_{\partial Z_1} g(z, \phi) G(\mathbf{x}, z, \xi, \zeta) d\sigma_\xi$$

is the propagating (entire) Herglotz function, and T^{-1} is the inverse transformation which relates the coefficients of the starting field in spherical coordinates to those in cylindrical coordinates. Other minimization problems might be considered instead, for example see Xu [9].

STEP THREE

In order to consider the case with an index of refraction which is depth dependent we must make certain alternations in STEP ONE and STEP TWO. In STEP ONE we need to replace the complete family (1.9) by another one, which must be solutions of the depth-dependent Helmholtz equation

$$\Delta u + k^2 n^2(z)u = 0. \quad (1.15)$$

Such a family may be generated by means of the transmutation

$$\Xi := \Omega(r, z, \phi) + \int_{z=z_0}^z K(z, s)\Omega(r, s, \phi)ds,$$

where the kernel $K(z,s)$ satisfies the Gelfand-Levitan equation

$$\frac{\partial^2 K}{\partial z^2} + \frac{\partial^2 K}{\partial s^2} + k^2[n^2(z) - 1]K = 0, \quad (1.16)$$

and the characteristic conditions [10]

$$2\frac{\partial}{\partial z}K(z, z) + k^2[n^2(z) - 1] = 0, \quad (1.17)$$

$$2\frac{\partial}{\partial z}K(z, -z + 2h) + k^2[n^2(z) - 1] = 0. \quad (1.18)$$

The functions $\Omega(r, z)$ are members from the family (1.9), where we have replaced the spherical coordinates (ρ, θ, ϕ) by the cylindrical coordinates (r, z, ϕ) .

In order to obtain the propagating field we replace the modal expansion (1.11) by

$$\sum_{n=0}^{N_2} \sum_{m=-M}^M \beta_{mn} \phi_n(z) H_m^1(ka_n r) e^{im\theta} \quad (1.19)$$

where the $\phi_n(z)$ are the modal solutions (eigenfunctions of the separated z -equation) for the variable index $n(z)$, and the λ_n are the corresponding eigenvalues, and $\nu_n = \sqrt{k^2 - \lambda_n^2}$. The modal solutions may be computed by transmutation, and we have developed a Fortran program which does exactly this. As mentioned above, the computational aspects of STEP THREE will be reported on in a later manuscript.

2 The Propagating Solution and its Far-field Pattern

Let $\mathbf{R}_b^3 = \{(\mathbf{x}, z); \mathbf{x} = (x_1, x_2) \in \mathbf{R}^2, 0 \leq z \leq h\}$ be a region corresponding to the finite depth ocean, where h is the ocean depth . Let Ω be an object

imbedded in \mathbf{R}_b^3 , which is a bounded, connected domain with C^2 boundary $\partial\Omega$ having an outward unit normal ν . If the object has a sound-soft boundary $\partial\Omega$, an incoming wave u^i , which incident on $\partial\Omega$, will be scattered to produce a scattered propagating wave u^s as well as its far-field pattern. This problem can be formulated as a Dirichlet boundary value problem for the scattering of time-harmonic acoustic waves in $\Omega_e := \mathbf{R}_b^3 \setminus \Omega$, namely to find a solution $u \in C^2(\mathbf{R}_b^3 \setminus \bar{\Omega}) \cap C(\mathbf{R}_b^3 \setminus \Omega)$ to the Helmholtz equation

$$\Delta_3 u + k^2 u = 0, \text{ in } \mathbf{R}_b^3 \setminus \bar{\Omega}, \quad (2.1)$$

such that u satisfies the boundary conditions

$$u = 0, \text{ as } z = 0, \quad (2.2)$$

$$\frac{\partial u}{\partial z} = 0, \text{ as } z = h, \quad (2.3)$$

$$u = 0, \text{ on } \partial\Omega. \quad (2.4)$$

Here k is a positive constant known as the wave number, $k \neq kh/\pi - 1/2$, and $u = u^i + u^s$, where u^i and u^s are the incident (entire) wave and the scattered wave respectively. The scattered wave has the modal representation

$$u^s = \sum_{n=0}^{\infty} \phi_n(z) u_n^s(\mathbf{x}), \quad (2.5)$$

where

$$\phi_n(z) = \sin[k(1 - a_n^2)^{\frac{1}{2}} z], \quad (2.6)$$

$$a_n = \left[1 - \frac{(2n+1)^2 \pi^2}{4k^2 h^2} \right]^{\frac{1}{2}}, \quad (2.7)$$

and the n^{th} mode of u^s , $u_n^s(\mathbf{x})$, satisfies the radiating condition

$$\lim_{r \rightarrow \infty} r^{\frac{1}{2}} \left(\frac{\partial u_n^s}{\partial r} - ika_n u_n^s \right) = 0, \quad r = |\mathbf{x}|, \quad n = 0, 1, \dots, \infty. \quad (2.8)$$

This problem is uniquely solvable [4]. The further properties of the solution can be found in [2] [3].

By the representation of u^s , we have [3]

$$u^s(\mathbf{x}, z) = \int_{\partial\Omega} \left(u^s \frac{\partial G}{\partial \nu} - G \frac{\partial u^s}{\partial \nu} \right) d\sigma, \quad (\mathbf{x}, z) \in \Omega_e, \quad (2.9)$$

and

$$0 = \int_{\partial\Omega} \left(u^i \frac{\partial G}{\partial \nu} - G \frac{\partial u^i}{\partial \nu} \right) d\sigma, \quad (\mathbf{x}, z) \in \Omega_e. \quad (2.10)$$

Here $G(z, \zeta, |\mathbf{x} - \xi|)$ is the Green's function in \mathbf{R}_b^3 , which has a normal mode representation

$$G(z, \zeta, |\mathbf{x} - \xi|) = \frac{i}{4} \sum_{n=0}^{\infty} \sum_{m=0}^{\infty} \frac{\epsilon_m \phi_n(z) \phi_n(\zeta)}{\|\phi_n\|^2} H_m^{(1)}(ka_n r) J_m(ka_n r') \\ [\cos(m\theta)\cos(m\theta') + \sin(m\theta)\sin(m\theta')]. \quad (2.11)$$

$$|\xi| = r' < r = |\mathbf{x}|.$$

and a ray representation

$$G(z, \zeta, |\mathbf{x} - \xi|) = \frac{e^{ik\sqrt{|\mathbf{x}-\xi|^2+(z-\zeta)^2}}}{4\pi\sqrt{|\mathbf{x}-\xi|^2+(z-\zeta)^2}} + \Phi_1(z, \zeta, |\mathbf{x} - \xi|), \quad (2.12)$$

where

$$\Phi_1(z, \zeta, |\mathbf{x} - \xi|) = \frac{1}{4\pi} \sum_{n=-\infty, n \neq 0}^{\infty} \left\{ \frac{e^{ik\sqrt{|\mathbf{x}-\xi|^2+(z-\zeta-2nh)^2}}}{\sqrt{|\mathbf{x}-\xi|^2+(z-\zeta-2nh)^2}} \right. \\ \left. - \frac{e^{ik\sqrt{|\mathbf{x}-\xi|^2+(z+\zeta-2nh)^2}}}{\sqrt{|\mathbf{x}-\xi|^2+(z+\zeta-2nh)^2}} \right\} - \frac{e^{ik\sqrt{|\mathbf{x}-\xi|^2+(z+\zeta)^2}}}{4\pi\sqrt{|\mathbf{x}-\xi|^2+(z+\zeta)^2}}$$

Here we denote (\mathbf{x}, z) in cylindrical coordinates by (r, θ, z) , and (ξ, ζ) by (r', θ', ζ) .

Recall that $u = u^i + u^s$ and $u|_{\partial\Omega} = 0$, then

$$\begin{aligned} u^s(\mathbf{x}, z) &= \int_{\partial\Omega} \left(u \frac{\partial G}{\partial \nu} - G \frac{\partial u}{\partial \nu} \right) d\sigma \\ &= - \int_{\partial\Omega} G \frac{\partial u}{\partial \nu} d\sigma, \quad (\mathbf{x}, z) \in \Omega_e, \end{aligned} \quad (2.13)$$

In view of the asymptotic behavior of Hankel's function and (2.11) we obtain the asymptotic formula (Compare (1.2), (1.3))

$$u^s(\mathbf{x}, z) = \frac{i}{2h} e^{-i\pi/4} \sum_{n=0}^N \left(\frac{2}{\pi k a_n r} \right)^{\frac{1}{2}} e^{i k a_n r} f_n(\theta, z, k) + O\left(\frac{1}{r^{\frac{3}{2}}}\right), \quad (2.14)$$

where

$$\begin{aligned} f_n(\theta, z, k) &= -\phi_n(z) \int_{\partial\Omega} \frac{\partial u(\xi, \zeta)}{\partial \nu_\xi} (e^{-i k a_n \mathbf{x} \cdot \xi} \phi_n(\zeta)) d\sigma_\xi, \\ \mathbf{x} &= (\cos\theta, \sin\theta). \end{aligned} \quad (2.15)$$

and where $[a]$ means the largest integer $\leq a$.

$$N = \left[\frac{2kh - \pi}{2\pi} \right]$$

Denote

$$V^N := L^2[0, 2\pi] \times \text{span}\{\phi_0, \phi_1, \dots, \phi_N\}, \quad (2.16)$$

we refer to the function $F(\theta, z, k) := \sum_{n=0}^N f_n(\theta, z, k) \in V^N$ as the representation of the propagating far-field pattern of the scattered wave.

3 A Numerical Scheme to Approximate the Starting Field

In order to detect the shape of a submersed object in a finite-depth ocean, we might bounce a “plane” wave off of it and then measure the wave scattered by the object. From these measurements we can reconstruct the shape of the object. For this purpose, we need to find efficient numerical procedures to construct a far-field pattern with respect to a given object and a given incoming waves. A problem in this approach is that the scattered acoustic waves are confined between the ocean floor and surface. The scattered wave may be decomposed into infinite number of normal modes, some of which propagate whereas the others evanesce. This fact makes it much more difficult to calculate the scattered wave and its far-field pattern than it was in the infinitely deep ocean.

Based on the representation formula (2.13) and the unique solvability of the exterior Dirichlet problem, we are led to consider a Fredholm integral equation of the second kind, namely [3]

$$\begin{aligned} \frac{\partial u(\mathbf{x}, z)}{\partial \nu_x} + 2 \int_{\partial \Omega} \left[\frac{\partial}{\partial \nu_x} G(z, \zeta, |\mathbf{x} - \xi|) + iG(z, \zeta, |\mathbf{x} - \xi|) \right] \frac{\partial u}{\partial \nu_\xi} d\sigma_\xi \\ = 2 \left[\frac{\partial u^i(\mathbf{x}, z)}{\partial \nu_x} + u^i(\mathbf{x}, z) \right] \end{aligned} \quad (3.1)$$

The Green’s function G can be represented as either (2.11) or (2.12).

By using a numerical integration scheme, we can solve this integral equation for $\frac{\partial u}{\partial \nu}$ to obtain a numerical print-out of (2.13) and (2.15). However, it is not difficult to see that this calculation is too time consuming to be practical. A more efficient numerical scheme is desirable. This may

be accomplished by using the asymptotic behavior of the Green's function $G(z, \zeta, | \mathbf{x} - \xi |)$ for points close to and far away from the object. To this end, we present a "matching" scheme in which the starting field and the propagating field are matched using a minimization procedure to obtain an approximate far-field pattern .

3.1 An approximation to the starting field

We assume that Ω is contained in a cylinder $D_a := \{(\mathbf{x}, z) \in \mathbf{R}_b^3, z_1 \leq z \leq z_2, | \mathbf{x} | \leq a\}$ where $\max \{z_2 - z_1, a\}$ is much smaller than h , the ocean depth. For (\mathbf{x}, z) close to Ω , for instance, $(\mathbf{x}, z) \in \partial D_a$, in view of (2.12), we know

$$G(z, \zeta, | \mathbf{x} - \xi |) \simeq \frac{e^{ik\sqrt{|\mathbf{x}-\xi|^2+(z-\zeta)^2}}}{4\pi\sqrt{|\mathbf{x}-\xi|^2+(z-\zeta)^2}}, \quad (3.2)$$

which, moreover, may be expanded as (cf. [5])

$$G(z, \zeta, | \mathbf{x} - \xi |) \simeq ik \sum_{n=0}^{\infty} \sum_{m=-n}^n j_n(k\rho) Y_n^m(\phi', \theta') h_n^1(kr) \overline{Y_n^m(\phi, \theta)}, \quad (3.3)$$

for $\rho < r$,

where we denote (\mathbf{x}, z) by (r, ϕ, θ) , (ξ, ζ) by (ρ, ϕ', θ') , $0 \leq \phi \leq \pi$, $0 \leq \theta \leq 2\pi$ and

$$Y_n^m(\phi, \theta) = \left[\frac{(2n+1)(n-|m|)!}{4\pi(n+|m|)!} \right]^{\frac{1}{2}} P_n^{|m|}(\cos\phi) e^{im\theta}, \quad (3.4)$$

are the surface harmonics.

Hence, for (r, ϕ, θ) close to $\partial\Omega$, we can express the starting field u^s as

$$\begin{aligned} u^s(\mathbf{x}, z) &= - \int_{\partial\Omega} G \frac{\partial u}{\partial \nu} d\sigma \\ &\simeq -ik \sum_{n=0}^{\infty} \sum_{m=-n}^n \alpha_{mn} h_n^1(kr) P_n^{|m|}(\cos\phi) e^{im\theta} \end{aligned} \quad (3.5)$$

where the α_{mn} are constants which are to be determined.

Now let u^i be a given incoming wave, with the representation

$$\begin{aligned} u^i(r, \theta, z) &= \sum_{n=0}^N c_n \phi_n(z) e^{ika_n r \cos(\theta - \alpha)} \\ &= \sum_{n=0}^N c_n \phi_n(z_0 + r \cos \phi) e^{ika_n r \sin \phi \cos(\theta - \alpha)}. \end{aligned} \quad (3.6)$$

Here N is $[(2kh - \pi)/2\pi]$, α is the given angle of incidence for the incoming wave, $0 \leq \alpha \leq 2\pi$, and the c_n ($n=0,1,\dots,N$) are given coefficients.

Since $u^i + u^s = 0$ on $\partial\Omega$, if we approximate u^s by u_a^s ,

$$u_a^s(\mathbf{x}, z) = \sum_{n=0}^{N_1} \sum_{m=-n}^n \alpha_{mn} h_n^1(kr) P_n^{|m|}(\cos \phi) e^{im\theta} \quad (3.7)$$

then the α_{mn} ($n = 0, 1, \dots, N_1$; $m = 0, \pm 1, \dots, \pm n$) can be approximated by the minimization procedure:

$$\min_{\alpha_{mn}} \|u^s - u^i\|_{V(\partial\Omega)}, \quad (3.8)$$

where $\|\cdot\|_{V(\partial\Omega)}$ is a suitable norm on $\partial\Omega$.

3.2 A program to determine the α_{mn}

In this section, we present a program to minimize (3.8) in the $L^2(\partial\Omega)$ norm, i.e.

$$J_1 := \min_{\alpha_{mn}} \int_{\partial\Omega} |u^s(\mathbf{x}, z) - u^i(\mathbf{x}, z)|^2 d\sigma. \quad (3.9)$$

Suppose Ω is starlike, i.e. that $\partial\Omega$ can be represented as

$$\mathbf{r} = \mathbf{r}(\theta, \phi), \quad 0 \leq \theta \leq 2\pi, \quad 0 \leq \phi \leq \pi; \quad (3.10)$$

then (3.9) becomes

$$J_1 := \min_{\alpha_{mn}} \int_0^\pi \int_0^{2\pi} |u^s(\mathbf{r}(\theta, \phi), \theta, \phi) - u^i(\mathbf{r}(\theta, \phi), \theta, \phi)|^2 r^2(\theta, \phi) \sin \phi d\theta d\phi. \quad (3.11)$$

Since

$$\begin{aligned}
& |u^s(\mathbf{r}(\theta, \phi), \theta, \phi) - u^i(\mathbf{r}(\theta, \phi), \theta, \phi)|^2 \\
&= \left| \sum_{n=0}^{N_1} \sum_{m=-n}^n \alpha_{mn} h_n^1(k\mathbf{r}) P_n^{|m|}(\cos\phi) e^{im\theta} - \right. \\
&\quad \left. \sum_{n=0}^N c_n \phi_n(z_0 + \mathbf{r}(\theta, \phi)\cos\phi) e^{ika_n \mathbf{r}(\theta, \phi) \sin\phi \cos(\theta-\alpha)} \right|^2 \\
&=: \left[\sum_{n=0}^{N_1} \sum_{m=-n}^n (\alpha_{mn}^1 A_{mn}^1 - \alpha_{mn}^2 A_{mn}^2) - B_1 \right]^2 \\
&\quad + \left[\sum_{n=0}^{N_2} \sum_{m=-n}^n (\alpha_{mn}^1 A_{mn}^2 + \alpha_{mn}^2 A_{mn}^1) - B_2 \right]^2,
\end{aligned}$$

where

$$\begin{aligned}
A_{mn}^1 &= \operatorname{Re}\{h_n^1(k\mathbf{r}(\theta, \phi)) P_n^{|m|}(\cos\phi) e^{im\theta}\}, \\
A_{mn}^2 &= \operatorname{Im}\{h_n^1(k\mathbf{r}(\theta, \phi)) P_n^{|m|}(\cos\phi) e^{im\theta}\}, \\
B_1 &= \operatorname{Re}\left\{ \sum_{n=0}^N c_n \phi_n(z_0 + \mathbf{r}(\theta, \phi)\cos\phi) e^{ika_n \mathbf{r}(\theta, \phi) \sin\phi \cos(\theta-\alpha)} \right\}, \\
B_2 &= \operatorname{Im}\left\{ \sum_{n=0}^N c_n \phi_n(z_0 + \mathbf{r}(\theta, \phi)\cos\phi) e^{ika_n \mathbf{r}(\theta, \phi) \sin\phi \cos(\theta-\alpha)} \right\}.
\end{aligned}$$

Here the c_n ($n = 0, 1, \dots, N$), are given complex numbers, α is a given real number, and $\mathbf{r}(\theta, \phi)$ is a real function for $0 \leq \theta \leq 2\pi$, $0 \leq \phi \leq \pi$.

Let us denote certain sums appearing above as

$$V_1(\theta, \phi) = \sum_{n=0}^{N_1} \sum_{m=-n}^n (\alpha_{mn}^1 A_{mn}^1 - \alpha_{mn}^2 A_{mn}^2) - B_1, \quad (3.12)$$

$$V_2(\theta, \phi) = \sum_{n=0}^{N_2} \sum_{m=-n}^n (\alpha_{mn}^1 A_{mn}^2 + \alpha_{mn}^2 A_{mn}^1) - B_2. \quad (3.13)$$

By using the numerical quadrature

$$\int_0^\pi \int_0^{2\pi} (\cdot) \mathbf{r}^2 \sin\phi d\theta d\phi = \frac{\pi^2}{JL} \left[\sum_{p=0}^J \sum_{q=0}^{2L-1} (\cdot) \mathbf{r}^2(\theta_q, \phi_p) \sin\phi_p \right], \quad (3.14)$$

we are then able to reformulate our minimization problem as

$$\begin{aligned}
J_1 &= \min_{\alpha_{mn}^1, \alpha_{mn}^2} \frac{\pi^2}{JL} \sum_{p=0}^J \sum_{q=0}^{2L-1} \{[V_1(\theta_q, \phi_p)]^2 + [V_2(\theta_q, \phi_p)]^2\} \mathbf{r}^2(\theta_q, \phi_p) \sin \phi_p \\
&=: \min_{\alpha_{mn}^1, \alpha_{mn}^2} \sum_{p=0}^J \sum_{q=0}^{2L-1} \{[f_1(\theta_q, \phi_p)]^2 + [f_2(\theta_q, \phi_p)]^2\}, \quad (3.15)
\end{aligned}$$

where

$$f_i(\theta_q, \phi_p) := \frac{\pi}{\sqrt{JL}} V_i(\theta_q, \phi_p) \mathbf{r}(\theta_q, \phi_p) \sqrt{\sin \phi_p}, \quad i = 1, 2. \quad (3.16)$$

In the next subsection we present a program to provide functions f_1 and f_2 . A minimization subroutine is then used to produce α_{mn}^1 and α_{mn}^2 , and hence,

$$\alpha_{mn} = \alpha_{mn}^1 + i\alpha_{mn}^2, \quad 0 \leq n \leq N_1, \quad -n \leq m \leq n$$

are found.

3.3 Some test examples

A Fortran program based on the above scheme has been written. (See appendix).

As a test for the starting field part of the program, we solve two problems with known boundary data and analytic solutions.

a) Let $h=10$, $k=2$, $\Omega = \{(\mathbf{x}, z); |\mathbf{x}|^2 + (z-5)^2 = 1\}$,

$$u^i = h_0^1(2)P_0^0(\cos \phi), \text{ on } \Omega$$

then the analytic solution is

$$u^s = h_0^1(2r)P_0^0(\cos \phi), \text{ for } r > 1;$$

i.e. $\alpha_{00} = 1$, $\alpha_{mn} = 0$, for $m \neq 0$ or $n \neq 0$.

The numerical result:

initial data	e=max	$ \beta_{mn} - \beta_{mn}^{exact} $
(a)		10^{-8}
(b)		10^{-8}

b) Let $h=20, k=2, \Omega = \{(\mathbf{x}, z); |\mathbf{x}|^2 + (z - 10)^2 = 1\}$,

$$u^i = h_1^1\left(\frac{\pi}{200}\right)P_1^0(\cos\phi) + h_2^1\left(\frac{\pi}{200}\right)P_2^1(\cos\phi)e^{i\theta}, \text{ on } \Omega$$

then the analytic solution is

$$u^s = h_1^1\left(\frac{\pi r}{200}\right)P_1^0(\cos\phi) + h_2^1\left(\frac{\pi r}{200}\right)P_2^1(\cos\phi)e^{i\theta}, \text{ for } r > 1$$

i.e. $\alpha_{01} = 1, \alpha_{12} = 1, \alpha_{mn} = 0$, for other m, n .

The numerical result:

initial data	e=max	$ \beta_{mn} - \beta_{mn}^{exact} $
(a)		10^{-8}
(b)		10^{-8}

4 A Numerical Scheme to Match the Starting Field with the Propagating Field

4.1 A minimization matching scheme

In view of (2.11), we know that for $|\mathbf{x}| > a_0$, where $a_0 = \min\{a : D_a \supset \Omega\}$, the scattered solution can be written as

$$\begin{aligned} u^s(\mathbf{x}, z) &= - \int_{\partial\Omega} G \frac{\partial u}{\partial \nu} d\sigma \\ &= \sum_{n=0}^{\infty} \sum_{m=-\infty}^{\infty} \beta_{mn} \phi_n(z) H_m^1(ka_n r) e^{im\theta} \end{aligned} \quad (4.1)$$

where $\beta_{mn} \in \mathbf{C}$, for $n = 0, 1, \dots, \infty$, $j = 0, \pm 1, \dots, \pm\infty$, are constants which might be computed from boundary data on $\partial\Omega$.

Instead of repeating the method of Section 3, we use a optimal scheme to determine β_{mn} by matching the “starting field” to the “propagating field” on a suitable surface Γ . Γ is chosen conveniently to lie in the intersection of the region corresponding to the starting field and propagating fields.

Suppose that Γ may be parametrized as $\{(r, \theta, z) : r = r(\theta, z), 0 \leq \theta \leq 2\pi, 0 \leq z \leq h\}$, from (3.7) we know that the starting field u^s scattered off Ω by an incoming wave u^i may be approximated by

$$\begin{aligned} u_a^s(\mathbf{x}, z) &= \sum_{n=0}^{N_1} \sum_{m=-n}^n \alpha_{mn} h_n^1(k\sqrt{r^2(\theta, z) + (z - z_0)^2}) \\ &P_n^{|m|} \left(\frac{z - z_0}{\sqrt{r^2(\theta, z) + (z - z_0)^2}} \right) e^{im\theta} \end{aligned} \quad (4.2)$$

$$0 \leq \theta \leq 2\pi, \quad 0 \leq z \leq h.$$

Here N_1 is a chosen positive number, and the α_{mn} have been determined in section 3.2.

Let u_p^s be an approximation to the propagating solution,

$$u_p^s(\mathbf{x}, z) = \sum_{n=0}^{N_2} \sum_{m=-M}^M \beta_{mn} \phi_n(z) H_m^1(ka_n r) e^{im\theta} \quad (4.3)$$

then

$$u_p^s(\mathbf{x}, z) \simeq u_a^s(\mathbf{x}, z), \quad \text{on } \Gamma. \quad (4.4)$$

Hence, we can determine β_{mn} by

$$\min_{\beta_{mn}} \| u_p^s(\mathbf{x}, z) - u_a^s(\mathbf{x}, z) \|_{V(\Gamma)}. \quad (4.5)$$

Again here $\| \cdot \|_{V(\Gamma)}$ is a suitable chosen norm on Γ . Since the approximate starting field is in all likelihood closer to the actual starting field when (\mathbf{x}, z) is near Ω and away from the oceansurface and bottom, this suggests we use a weighted norm to emphasize those points near Ω .

Recall that we assumed that $\Omega \subset D_a = \{(\mathbf{x}, z) \in R_b^3, z_1 \leq z \leq z_2, |\mathbf{x}| \leq a\}$; hence, we consider the minimization problem with weighted L^2 -norm

$$\min \int_0^h \int_0^{2\pi} |s_p^s(\mathbf{x}, z) - s_a^s(\mathbf{x}, z)|^2 w(z, \theta) r(\theta, z) d\theta dz, \quad (4.6)$$

where $w(z)$ is chosen to emphasize points near Ω . If we choose Γ to be the cylinder

$$\Gamma := \{(r, \theta, z); r = a, 0 \leq \theta \leq 2\pi, 0 \leq z \leq h\},$$

and the weight to be given as

$$w(z, \theta) = \begin{cases} 1 & \text{if } z_1 \leq z \leq z_2 \\ 0 & \text{if } 0 \leq z \leq z_1, \text{ or } z_2 \leq z \leq h, \end{cases}$$

the situation is quite easily implimented. A slightly more complicated situation is to choose w as a discrete measure having points concentrated near

Ω . Discretizing (3.6) then leads to the problem

$$F(\alpha) := \min_{\beta_{mn}} \left\{ \frac{\pi h}{m_1 m_2} \sum_{q=0}^{m_1} \sum_{p=0}^{m_2} r(\theta_p, z_q) w(\theta_p, z_q) \right. \\ \left. \left| \sum_{n=0}^{N_2} \sum_{m=-M}^M \beta_{mn} \phi_n(z_q) H_m^{(1)}(ka_n r) e^{im\theta_p} \right. \right. \\ \left. \left. - \sum_{n=0}^{N_1} \sum_{m=-n}^n \alpha_{mn} h_n^{(1)}(k\sqrt{r^2 + (z_q - z_0)^2}) P_n^{|m|} \left(\frac{z_q - z_0}{\sqrt{r^2 + (z_q - z_0)^2}} \right) e^{im\theta_p} \right|^2 \right\} \quad (4.7)$$

where $(r(\theta_p, z_q), \theta_p, z_q)$ are points on the matching surface.

Let

$$C_1(\theta_p, z_q) := \operatorname{Re} \left\{ \sum_{n=0}^{N_1} \alpha_{mn} h_n^{(1)}(k\sqrt{r^2 + (z_q - z_0)^2}) \right. \\ \left. P_n^{|m|} \left(\frac{z_q - z_0}{\sqrt{r^2 + (z_q - z_0)^2}} \right) e^{im\theta_p} \right\} \quad (4.8)$$

$$C_2(\theta_p, z_q) := \operatorname{Im} \left\{ \sum_{n=0}^{N_1} \alpha_{mn} h_n^{(1)}(k\sqrt{r^2 + (z_q - z_0)^2}) \right. \\ \left. P_n^{|m|} \left(\frac{z_q - z_0}{\sqrt{r^2 + (z_q - z_0)^2}} \right) e^{im\theta_p} \right\} \quad (4.9)$$

A straightforward calculation shows that

$$\begin{aligned} & \operatorname{Re} \{ \beta_{mn} \phi_n(z_q) H_m^{(1)}(ka_n r) e^{im\theta_p} \} \\ &= \{ \beta_{mn}^1 [J_m(ka_n r) \cos m\theta_p - Y_m(ka_n r) \sin m\theta_p] \\ & - \beta_{mn}^2 [Y_m(ka_n r) \cos m\theta_p + J_m(ka_n r) \sin m\theta_p] \} \phi_n(z_q) \\ & \operatorname{Im} \{ \beta_{mn} \phi_n(z_q) H_m^{(1)}(ka_n r) e^{im\theta_p} \} \\ &= \{ \beta_{mn}^1 [Y_m(ka_n r) \cos m\theta_p + J_m(ka_n r) \sin m\theta_p] \\ & + \beta_{mn}^2 [J_m(ka_n r) \cos m\theta_p - Y_m(ka_n r) \sin m\theta_p] \} \phi_n(z_q) \end{aligned}$$

Denoting

$$U_{mn}(\theta_p, z_q) := J_m(ka_n r(\theta_p, z_q)) \cos m\theta_p - Y_m(ka_n r(\theta_p, z_q)) \sin m\theta_p \quad (4.10)$$

$$V_{mn}(\theta_p, z_q) := Y_m(ka_n r(\theta_p, z_q)) \cos m\theta_p + J_m(ka_n r(\theta_p, z_q)) \sin m\theta_p \quad (4.11)$$

for $m = -M, \dots, -1, 0, 1, \dots, M$; $n = 0, 1, \dots, N_2$

($p = 0, 1, \dots, m_2$; $q = 0, 1, \dots, m_1$)

then leads to

$$\begin{aligned} F(\alpha) &= \min_{\beta_{mn}} \left\{ \frac{\pi h}{m_1 m_2} \sum_{q=0}^{m_1} \sum_{p=0}^{m_2} r(\theta_p, z_q) w(\theta_p, z_q) \right. \\ &\quad \left[\left(\sum_{n=0}^{N_2} \sum_{m=-M}^M (\beta_{mn}^1 U_{mn}(\theta_p, z_q) - \beta_{mn}^2 V_{mn}(\theta_p, z_q)) \phi_n(z_q) - C_1(\theta_p, z_q) \right)^2 \right. \\ &\quad \left. \left. + \left(\sum_{n=0}^{N_2} \sum_{m=-M}^M (\beta_{mn}^1 V_{mn}(\theta_p, z_q) + \beta_{mn}^2 U_{mn}(\theta_p, z_q)) \phi_n(z_q) - C_2(\theta_p, z_q) \right)^2 \right] \right\} \\ &=: \min_{\beta_{mn}^1, \beta_{mn}^2} \sum_{q=0}^{m_1} \sum_{p=0}^{m_2} \{ [g_1(\theta_p, z_q)]^2 + [g_2(\theta_p, z_q)]^2 \}, \end{aligned} \quad (4.12)$$

where

$$g_1(\theta_p, z_q) = \left[\frac{\pi h}{m_1 m_2} r(\theta_p, z_q) w(\theta_p, z_q) \right]^{1/2}$$

$$\left[\sum_{n=0}^{N_2} \sum_{m=-M}^M (\beta_{mn}^1 U_{mn}(\theta_p, z_q) - \beta_{mn}^2 V_{mn}(\theta_p, z_q)) \phi_n(z_q) - C_1(\theta_p, z_q) \right] \quad (4.13)$$

$$g_2(\theta_p, z_q) = \left[\frac{\pi h}{m_1 m_2} r(\theta_p, z_q) w(\theta_p, z_q) \right]^{1/2}$$

$$\left[\sum_{n=0}^{N_2} \sum_{m=-M}^M (\beta_{mn}^1 V_{mn}(\theta_p, z_q) + \beta_{mn}^2 U_{mn}(\theta_p, z_q)) \phi_n(z_q) - C_2(\theta_p, z_q) \right] \quad (4.14)$$

By calling the minimization subroutine, we compute β_{mn}^1 and β_{mn}^2 , and hence also

$$\beta_{mn} = \beta_{mn}^1 + i\beta_{mn}^2, \quad 0 \leq n \leq N_2, \quad -M \leq m \leq M.$$

4.2 numerical examples

A Fortran program for the above matching scheme has been developed (see Appendix). In order to test the accuracy and capability of the program, we have done some numerical tests.

4.2.1 The following two test problem are exact solutions with given boundary data on the matching cylinder, which can be thought of as the data produced by some starting field. By choosing different initial guesses, the output of the tests are exactly the same. This shows that our program is dependable in the matching step.

Example 1: Let $h=10$, $k=2$, and the matching surface $\Gamma = \{(r, \theta, z); r = 12, 0 \leq \theta \leq 2\pi, 0 \leq z \leq h\}$. The starting field has the known data on Γ as:

$$u_a^s(\mathbf{x}, z) = H_0^1(ka_0r_0)\phi_0(z), \quad 0 \leq z \leq 10$$

where $a_0 = [1 - \pi^2/(4k^2h^2)]^{1/2}$, $r_0 = 12$. The analytic solution to this problem is

$$u^s(\mathbf{x}, z) = H_0^1(ka_0r)\phi_0(z), \quad r \geq 12, \quad 0 \leq z \leq 10$$

i.e. $\beta_{00} = 1$, $\beta_{mn} = 0$ for other m, n .

By choosing $N_2 = 3$, $M = 2$, $m_1 = 5$, $m_2 = 10$, and using a different initial guess

(a) $\beta_{mn}^i = 1$;

(b) $\beta_{00} = 0$, $\beta_{mn}^i = 1$ for other m, n .

we get the following output result:

initial data	e=max	$ \beta_{mn} - \beta_{mn}^{exact} $
(a)		10^{-8}
(b)		10^{-8}

Example 2: Let $h=10, k=2$, and the matching surface $\Gamma = \{(r, \theta, z); r = 10, 0 \leq \theta \leq 2\pi, 0 \leq z \leq h\}$. The starting field has the known data on Γ as:

$$u_a^s(\mathbf{x}, z) = H_1^{(1)}(ka_1 r)\phi_1(z)e^{i\theta} + H_0^{(1)}(ka_2 r)\phi_2(z), \quad 0 \leq \theta \leq 2\pi, \quad 0 \leq z \leq 10$$

The analytic solution to this problem is

$$u_a^s(\mathbf{x}, z) = H_1^1(ka_1 r)\phi_1(z)e^{i\theta} + H_0^1(ka_2 r)\phi_2(z),$$

$$0 \leq \theta \leq 2\pi, \quad 0 \leq z \leq 10, \quad r > 0.$$

i.e.

$$\beta_{11} = 1;$$

$$\beta_{20} = 1.$$

Test result:

initial data	e=max	$ \beta_{mn} - \beta_{mn}^{exact} $
(a)		10^{-8}
(b)		10^{-8}

5 Some examples of the approximate propagating far-field pattern

As shown in the previous section, an approximate propagating field can be written as:

$$u^s(\mathbf{x}, z) \simeq \sum_{n=0}^{N_2} \sum_{m=-M}^M \beta_{mn} \phi_n(z) H_m^{(1)}(ka_n r) e^{im\theta} \quad (5.1)$$

for $r \geq a_0$.

where $N_2 \geq N$ and N is the number of propagating modes. Now let $r \rightarrow \infty$, we will approximate the propagating far-field pattern from the above formula. It is well known that $H_m^{(1)}(ka_n r)$ has the asymptotic behavior

$$H_m^{(1)}(ka_n r) = \left(\frac{2}{k\pi a_n r}\right)^{1/2} e^{-i(m+\frac{1}{2})\frac{\pi}{2}} e^{ika_n r} + O\left(\frac{1}{r^{3/2}}\right), \quad (5.2)$$

as $r \rightarrow \infty$, for $n = 0, 1, \dots, N$;

$$H_m^{(1)}(ka_n r) = O\left(\frac{e^{-k|a_n|r}}{r^{1/2}}\right), \quad (5.3)$$

as $r \rightarrow \infty$, for $n > N$.

Hence,

$$u^s(\mathbf{x}, z) \simeq \sum_{n=0}^{N_2} \sum_{m=-M}^M \beta_{mn} \left(\frac{2}{k\pi a_n r}\right)^{1/2} e^{-i(m+\frac{1}{2})\frac{\pi}{2}} e^{ika_n r} \phi_n(z) e^{im\theta} + O\left(\frac{1}{r^{3/2}}\right), \quad \text{as } r \rightarrow \infty. \quad (5.4)$$

In view of (2.14), the approximate propagating far-field pattern is

$$\begin{aligned} F(\theta, z, k) &:= \sum_{n=0}^N f_n(\theta, z, k) \\ &= \sum_{n=0}^N \sum_{m=-M}^M \beta_{mn} \left(\frac{i}{2h}\right)^{-1} e^{-i\frac{m\pi}{2}} \phi_n(z) e^{im\theta} \end{aligned} \quad (5.5)$$

5.1 Some numerical examples of far-field pattern

Now we present some numerical examples from our computation. Figure 1 and Figure 2 show a comparison of the theoretical result and computational result for a simple scatterer – cylinder. Figure 3 and Figure 4 shows the far field patterns of two special objects that can be represented as $r = r(\theta, z) > 0$ for $0 \leq \theta \leq 2\pi, 0 \leq z \leq h$. These far field patterns are using in an inverse scattering problem to recover the shapes of the objects. [10]

Figure 5 to Figure 12 are examples of far field patterns. They will be used in our investigation of under water inverse scattering problem as input data.

References

- [1] Ahluwalia, D. and Keller, J.; "Exact and asymptotic representations of the sound field in a stratified ocean," *Wave Propagation and Underwater Acoustics*, Lecture Notes in Physics 70, Springer, Berlin (1977)
- [2] Brekhovskikh, L. ; *Wave in Layered Media*, 2nded., Academic Press, New York, (1980)
- [3] Colton, D. and Kress, R.; *Integral Equation Methods in Scattering Theory*, John Wiley, New York, (1983)
- [4] Colton, D. and Monk, P.; "A novel method of solving the inverse scattering problem for time-harmonic acoustic waves in the resonance region," *SIAM J. Appl. Math.* 45 (1985), 1039-1053.
- [5] Colton, D. and Monk, P.; "A novel method of solving the inverse scattering problem for time-harmonic acoustic waves in the resonance region : II." *SIAM J. Appl. Math.* 46 (1986), 506-523.
- [6] Duston, M., Gilbert, R.P., Verma, G.H. and Wood, D.H.; " Direct generation of normal modes by transmutation theory ", *Computational Acoustics: Algorithms and Applications*, Vol.2. (1987) 389-402
- [7] Gilbert, R.P. and Wood, D.H.; "A transmutational approach to underwater sound propagation", *Wave Motion* 8 (1986) 383-397.
- [8] Gilbert, R. P. and Xu, Y.; "Starting fields and far fields in ocean acoustics" ,*Wave Motion*, to appear, (1989)
- [9] Gilbert, R. P. and Xu, Yongzhi; "Dense sets and the projection theorem for acoustic harmonic waves in homogeneous finite depth ocean",*Mathematical*

Methods in the Applied Sciences, to appear, (1989)

[10] Xu, Yongzhi; “The propagating solution and far field patterns for acoustic harmonic waves in a finite depth ocean,” *Applicable Analysis*, to appear, (1989).

[11] Xu, Yongzhi; “An injective far-field pattern operator and inverse scattering problem in a finite depth ocean”, pre-print, (1988)

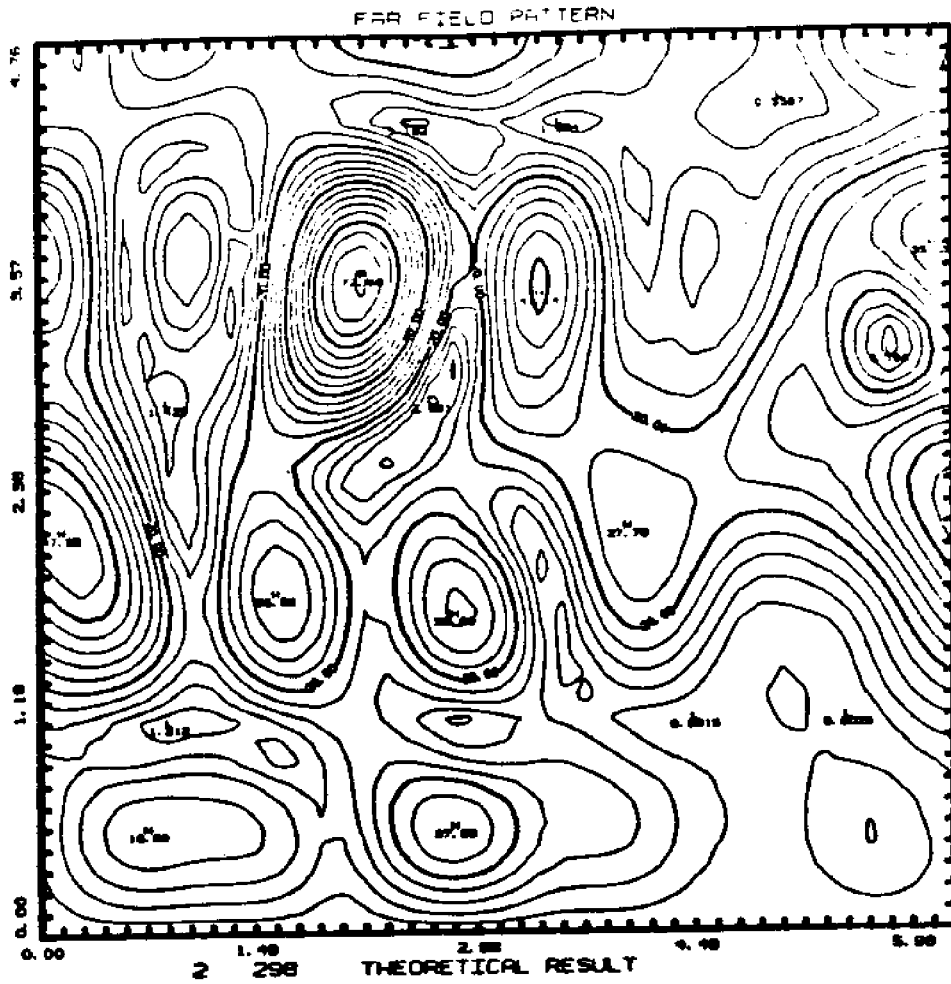


Figure 1:

Object:

$$r = 5, 0 \leq z \leq h, 0 \leq \theta \leq 2\pi;$$

Incoming wave:

$$u^i = \sum_{n=0}^5 \sum_{m=-3}^3 i^m J_m(ka_n r) \phi_n e^{im\theta};$$

$$k = 4.084, h = 5;$$

Theoretical far field pattern:

$$F(z, \theta) = \sum_{n=0}^5 \sum_{m=-3}^3 \frac{i^m J_m(5ka_n)}{H_m^{(1)}(5ka_n)} \left(\frac{i}{2h}\right)^{-1} e^{-im\pi/2} \phi_n(z) e^{im\theta},$$

$$0 \leq z \leq h, 0 \leq \theta \leq 2\pi.$$

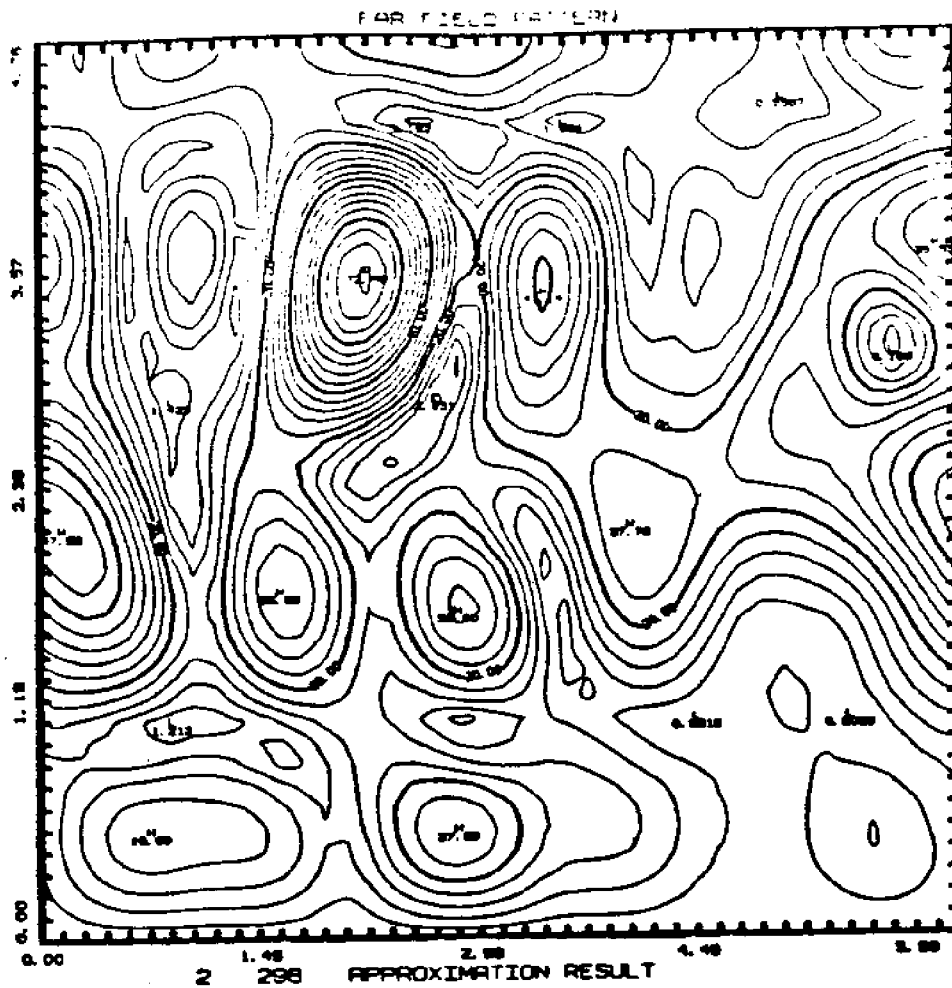


Figure 2:

Object:

$$r = 5, 0 \leq z \leq h, 0 \leq \theta \leq 2\pi;$$

Incoming wave:

$$u^i = \sum_{n=0}^{\infty} \sum_{m=-3}^3 i^m J_m(ka_n r) \phi_n e^{im\theta};$$

$$k = 4.084, h = 5;$$

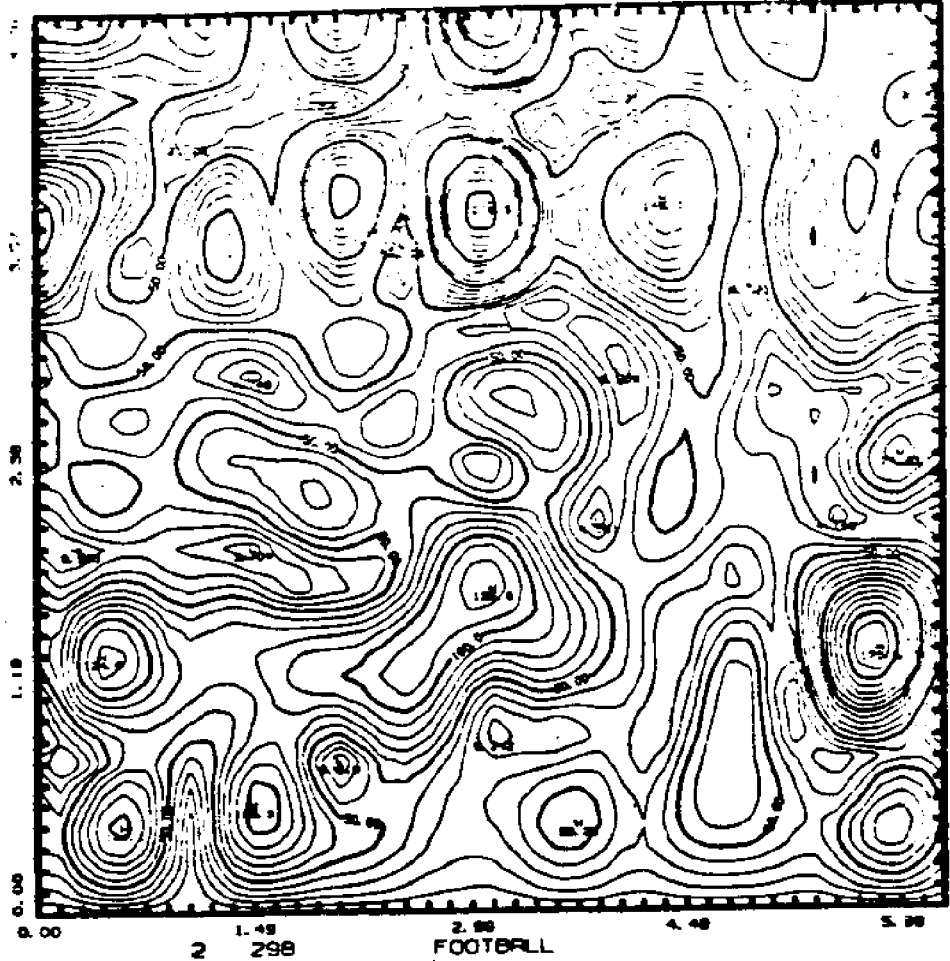


Figure 3:
Object:

$$r = 5 \sin(\pi z/h) + 2, \quad 0 \leq z \leq h, \quad 0 \leq \theta \leq 2\pi;$$

Incoming wave:

$$u^i = \sum_{n=0}^5 \sum_{m=-3}^3 i^m J_m(k a_n r) \phi_n e^{im\theta};$$

$$k = 4.084, \quad h = 5;$$

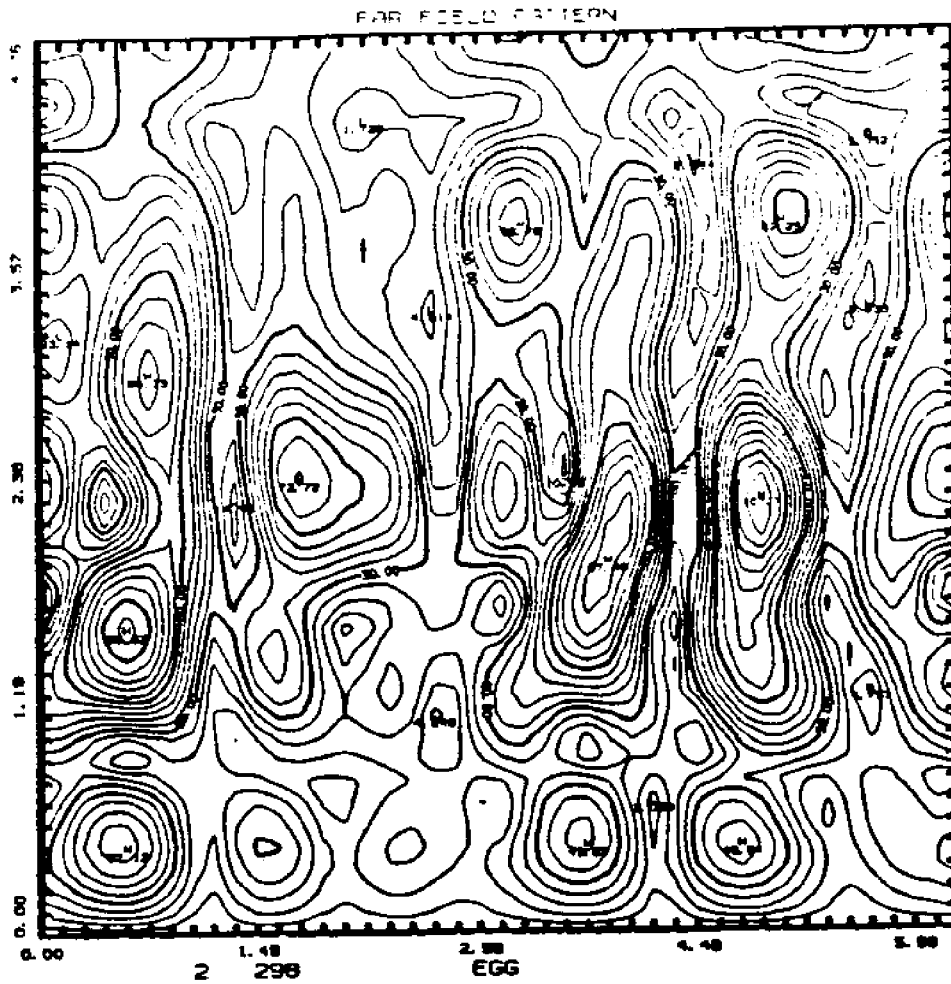


Figure 4:
Object:

$$r = 5z(h - z)/16 + 3, \quad 0 \leq z \leq h, \quad 0 \leq \theta \leq 2\pi;$$

Incoming wave:

$$u^i = \sum_{n=0}^5 \sum_{m=-3}^3 i^m J_m(ka_n r) \phi_n e^{im\theta};$$

$$k = 4.084, \quad h = 5;$$

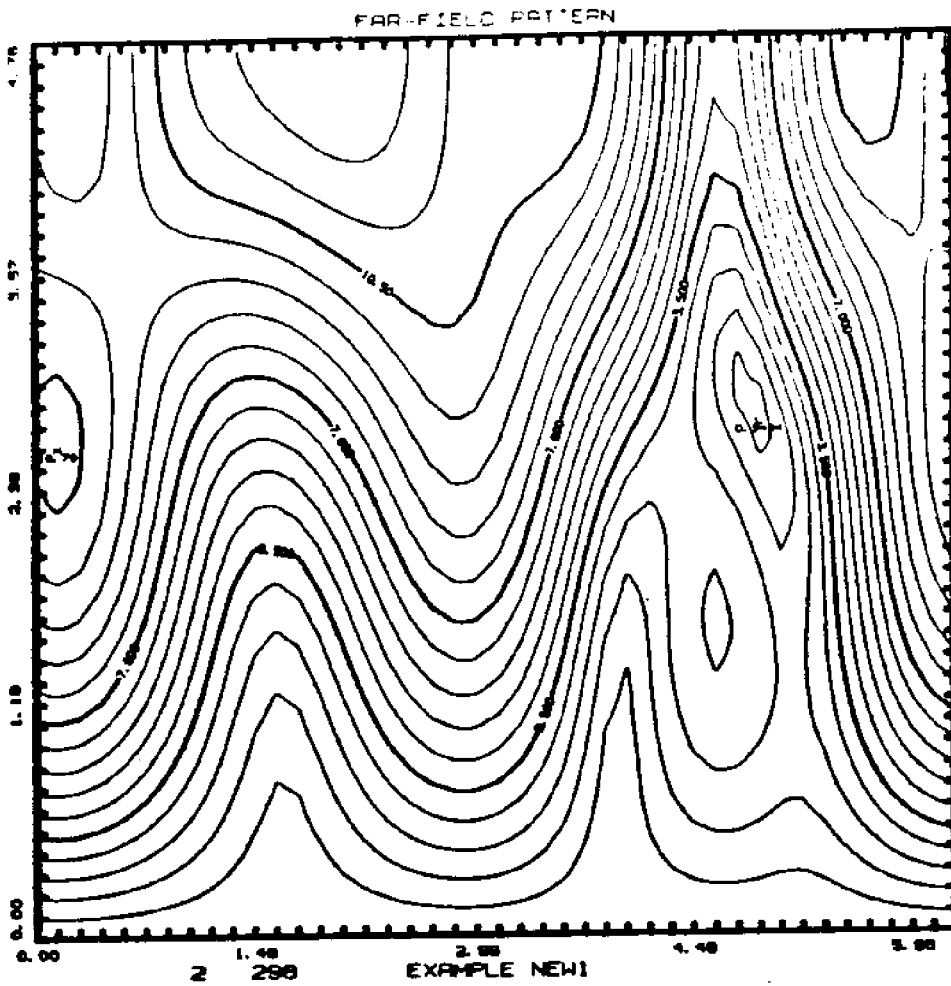


Figure 5:
Object:

$$\rho = 0.125(2 - \cos^2 \psi), \quad 0 \leq \psi \leq \pi, \quad 0 \leq \theta \leq 2\pi;$$

Incoming wave:

$$u^i = 5\phi_3 e^{ikz_3 \cos(\theta)};$$

$$k = 2.7, \quad h = 5, \quad z_0 = 2.5.$$

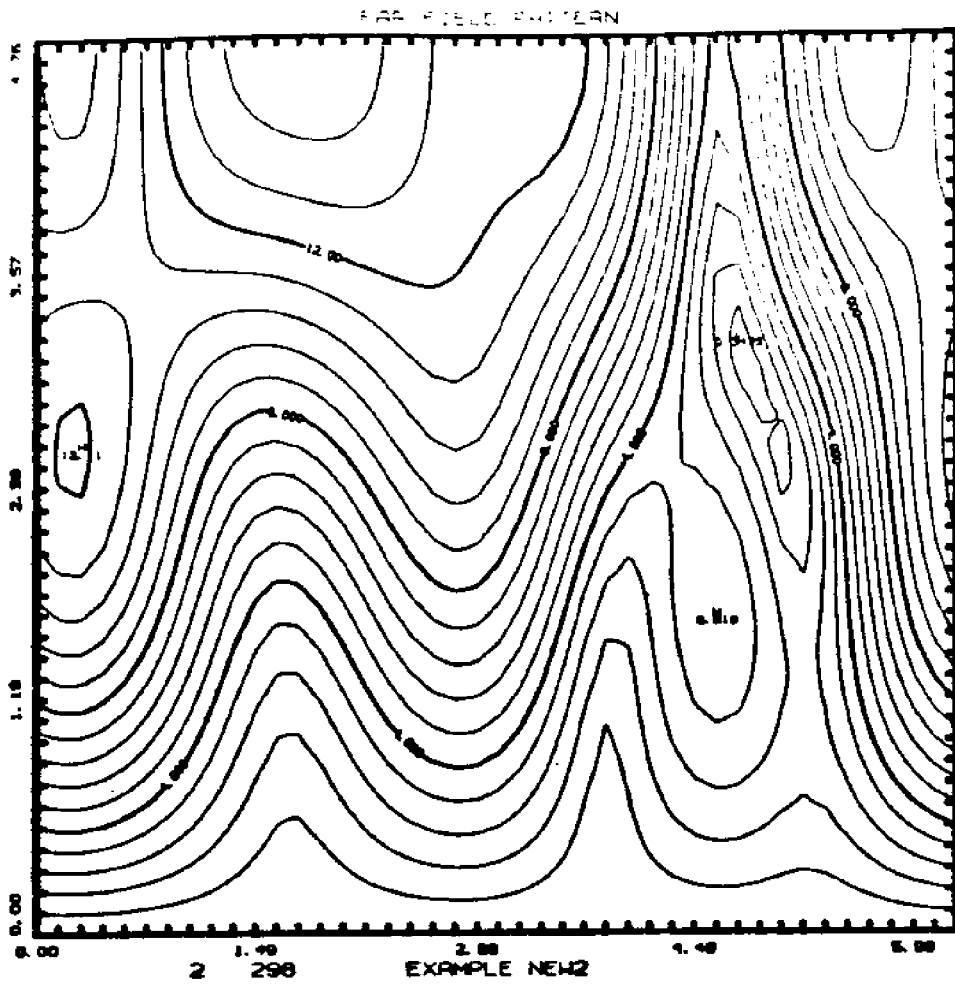


Figure 6:
Object:

$$\rho = 0.125(2 - \cos^2 \psi)(2 - \cos^2 \theta), \quad 0 \leq \psi \leq \pi, \quad 0 \leq \theta \leq 2\pi; \quad 0 \leq \theta \leq 2\pi$$

Incoming wave:

$$u^i = 5\phi_0 e^{iks_0 r \cos(\theta)};$$

$$k = 2.7, \quad h = 5, \quad z_0 = 2.5.$$

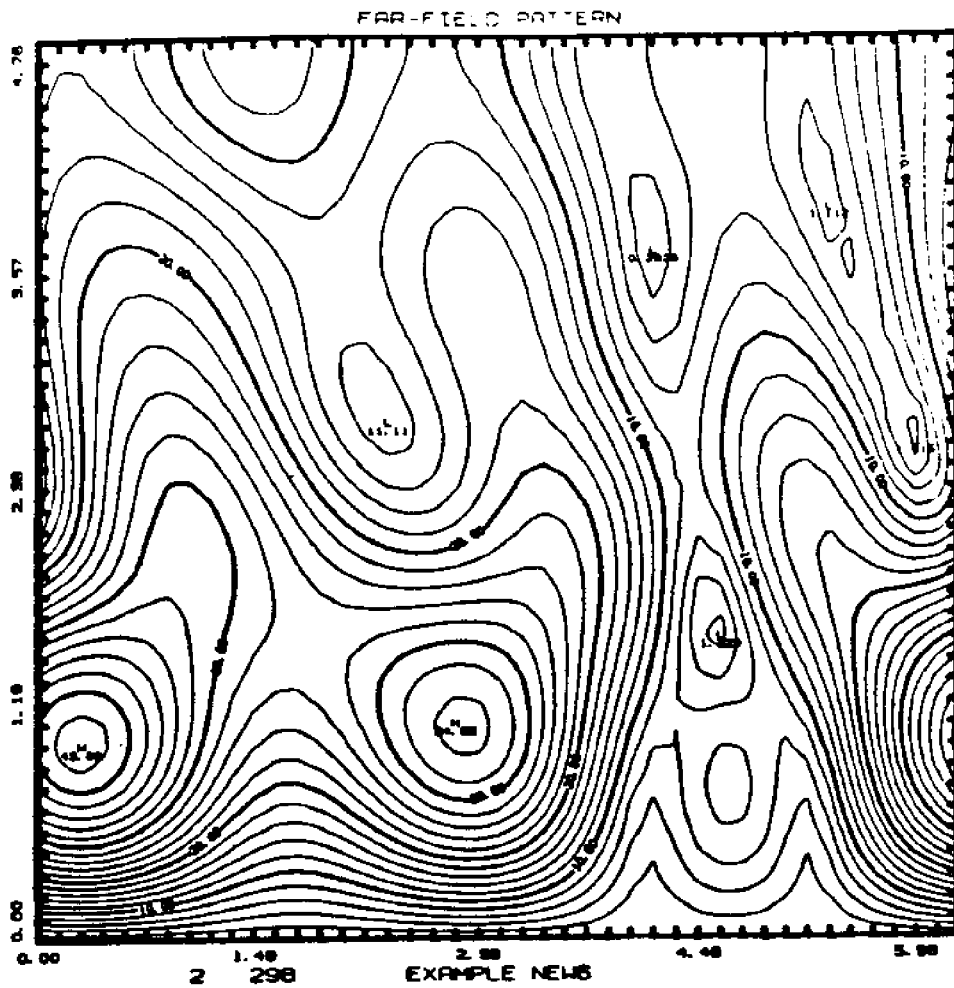


Figure 7:
Object:

$$\rho = 0.125(2 - \cos^2 \psi), \quad 0 \leq \psi \leq \pi, \quad 0 \leq \theta \leq 2\pi;$$

Incoming wave:

$$u^i = 5\phi_0 e^{ik_0 r \cos(\theta)},$$

$$k = 2.7, \quad h = 5, \quad z_0 = 2.5.$$

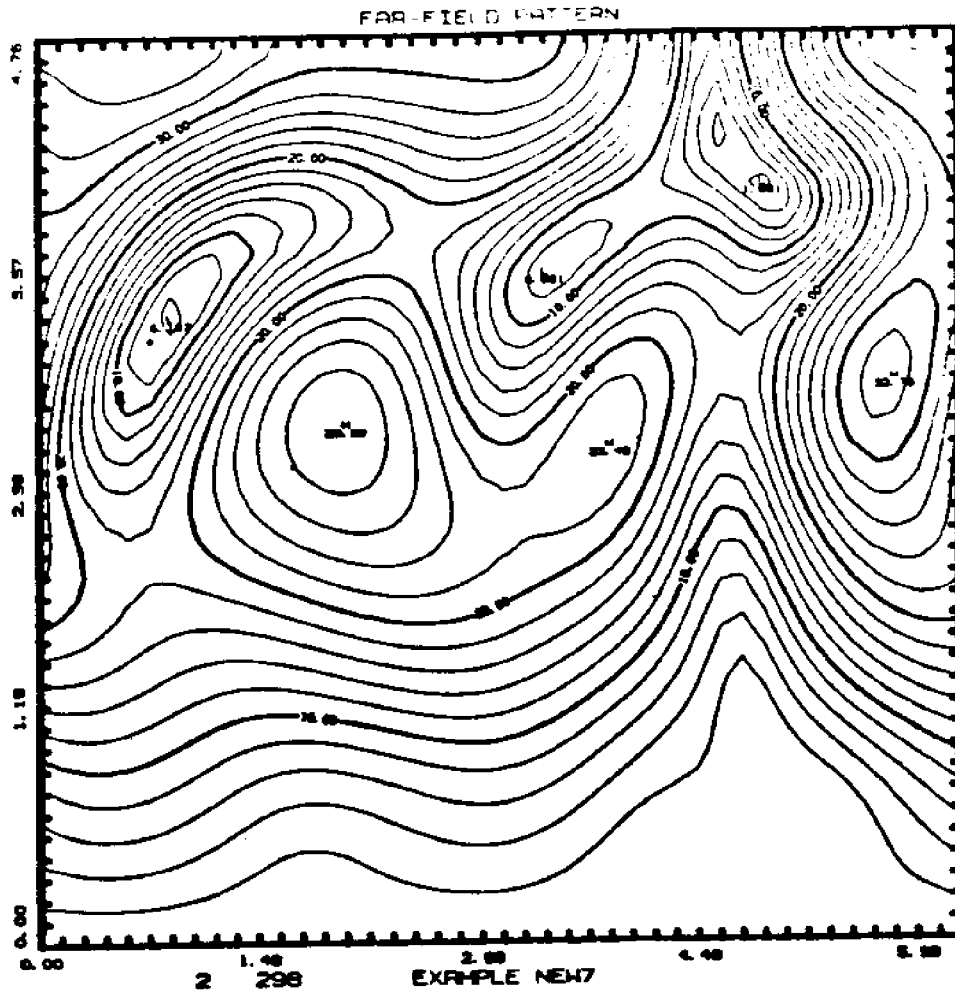


Figure 8:
Object:

$$\rho = 0.125(2 - \cos^2 \psi), \quad 0 \leq \psi \leq \pi, \quad 0 \leq \theta \leq 2\pi;$$

Incoming wave:

$$u^i = 5\phi_1 e^{ik_0 r \cos(\theta)};$$

$$k = 2.7, \quad h = 5, \quad z_0 = 2.5.$$

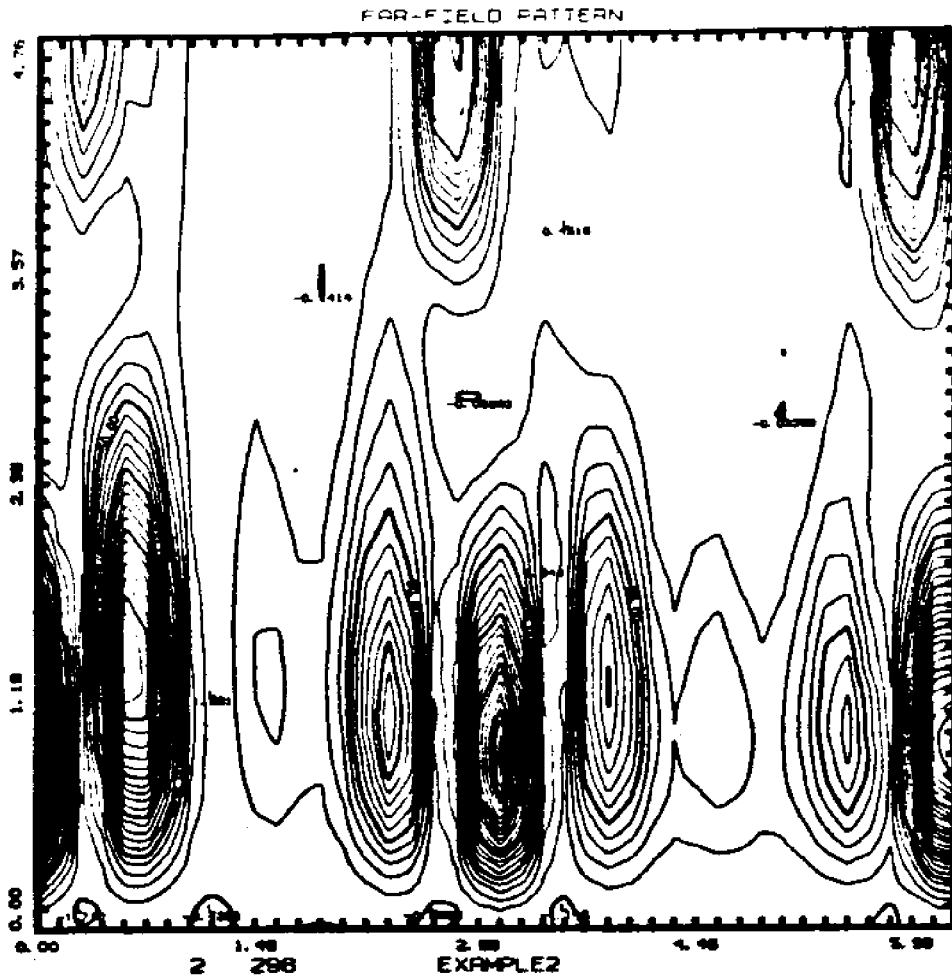


Figure 9:

Object:

$$\rho = 1, 0 \leq \psi \leq \pi, 0 \leq \theta \leq 2\pi;$$

Incoming wave:

$$u^i = \sum_{n=0}^7 \phi_n e^{ika_n r \cos(\theta - 1.2345)},$$

$$k = 5.34, h = 5, z_0 = 2.5.$$

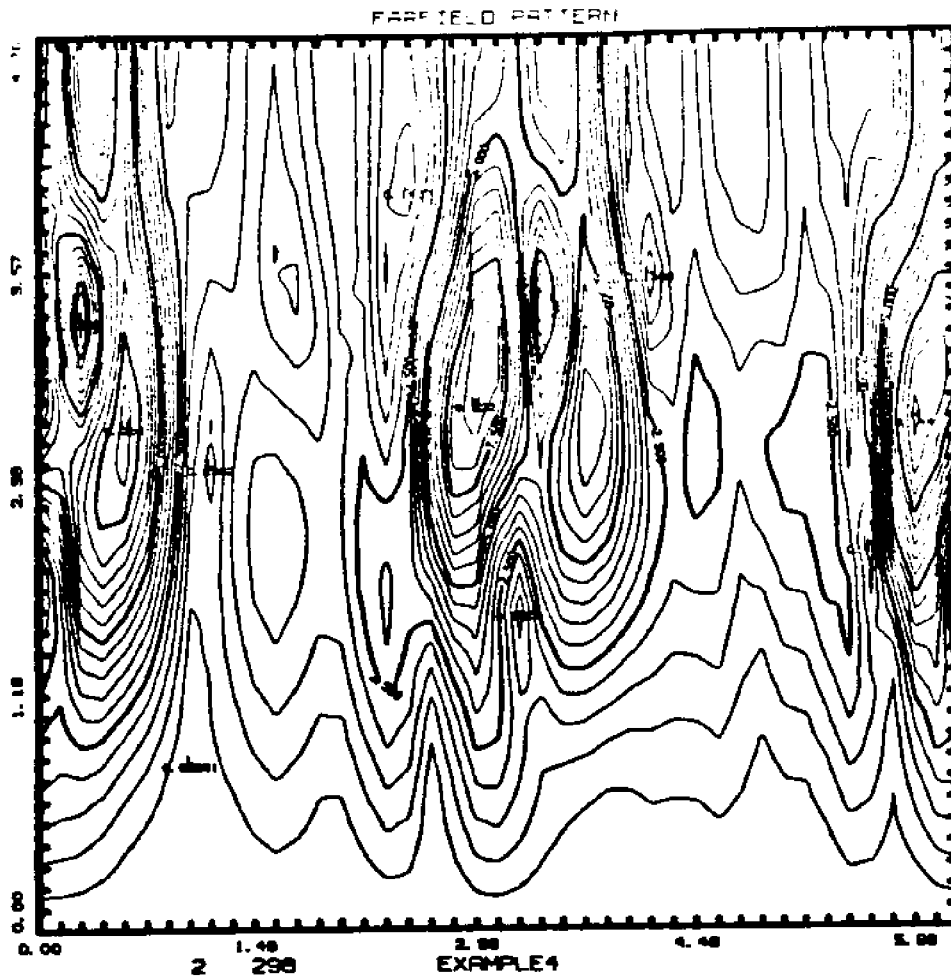


Figure 10:
Object:

$$\rho = 0.125(2 - \cos^2\theta), \quad 0 \leq \theta \leq 2\pi, \quad 0 \leq \theta \leq 2\pi;$$

Incoming wave:

$$u^i = \sum_{n=0}^7 \phi_n e^{ika_n r \cos(\theta - 1.2345)};$$

$$k = 5.34, \quad h = 5, \quad z_0 = 2.5.$$

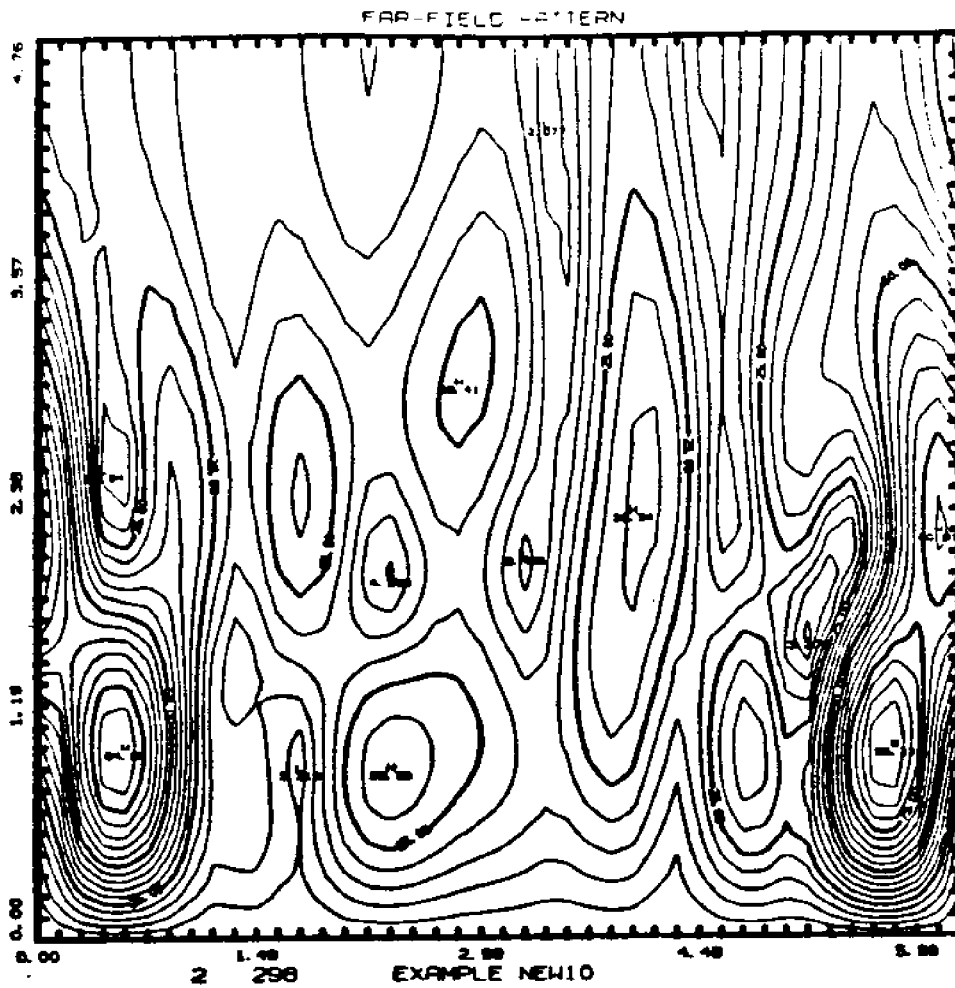


Figure 11:
Object:

$$\rho = 0.5(2 - \cos^2 \psi), \quad 0 \leq \psi \leq \pi, \quad 0 \leq \theta \leq 2\pi;$$

Incoming wave:

$$u^i = 5\phi_5 e^{ik_0 r \cos(\theta - \pi/2)},$$

$$k = 4.06, \quad h = 5, \quad z_0 = 2.5.$$

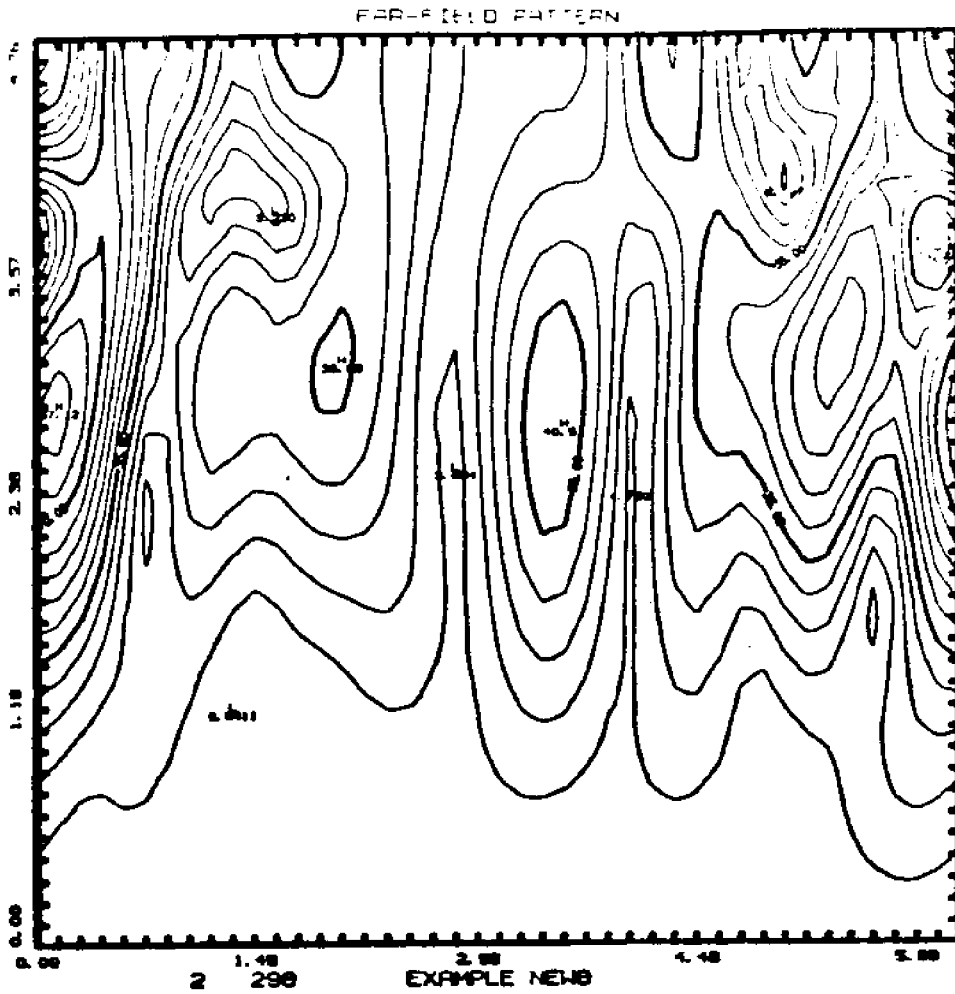


Figure 12:
Object:

$$\rho = 0.5(2 - \cos^2 \psi), \quad 0 \leq \psi \leq \pi, \quad 0 \leq \theta \leq 2\pi;$$

Incoming wave:

$$u^i = 5\phi_s e^{ikz_0 \cos(\theta)},$$

$$k = 4.06, \quad h = 5, \quad z_0 = 2.5.$$